PAPER • OPEN ACCESS

Temperature dependent structural evolution in nickel/carbon nanotube composites processed by high-pressure torsion

To cite this article: Andreas Katzensteiner *et al* 2017 *IOP Conf. Ser.: Mater. Sci. Eng.* **194** 012019

View the article online for updates and enhancements.

Related content

- Evolution of the microstructure in carbon nanotube reinforced Nickel matrix composites processed by high-pressure torsion

- Microstructural evolution in immiscible alloys processed by High-Pressure Torsion

- Comprehensive defect characterization of different iron samples after severe plastic deformation

Recent citations

- On the reinforcement homogenization in CNT/metal matrix composites during severe plastic deformation
  Katherine Aristizabal *et al*

Temperature dependent structural evolution in nickel/carbon nanotube composites processed by high-pressure torsion

Andreas Katzensteiner[1], Katherine Aristizabal[2], Sebastian Suarez[2], Reinhard Pippan[1] and Andrea Bachmaier[1]

[1] Erich Schmid Institute, Jahnstr. 12, A-8700 Leoben, Austria
[2] Department of Materials Science, Campus D3.3, D-66123 Saarbrücken, Germany

E-mail: `andreas.katzensteiner@oeaw.ac.at, katherine.aristizabal@uni-saarland.de,`
`s.suarez@mx.uni-saarland.de, reinhard.pippan@oeaw.ac.at,`
`andrea.bachmaier@oeaw.ac.at`

Abstract. Nickel/Carbon nanotube (CNT) composites with varying amounts of CNTs were processed at different temperatures by high-pressure torsion (HPT) with the aim to optimize the process parameters to obtain a homogenous dispersion of CNTs in the metallic matrix. As the CNT distribution has an enormous influence on the composite properties, the structural evolution with increasing strain and the final microstucture of the composites are investigated by scanning and transmission electron microscopy. Microhardness measurements were additionally performed. Microhardness increases up to 800 Vickers (HV) and the mean grain size decreases to an equivalent radius smaller than 40 nm for HPT at room temperature (RT), while the CNTs form rather large agglomerates. HPT deformation at 200°C shows no significant change in hardness, grain size and CNT agglomerate size. For HPT deformation at 300°C and 400°C grain sizes increase to 60 nm respectively 90 nm, microhardness decreases to 500 HV respectively 400 HV and the size of the CNT agglomerates decreases from more than 5 times the grain size at RT to smaller than the grain size. It could be shown that the optimal HPT processing route to improve the CNT distribution is a combination of deformation at 400°C with subsequent deformation at RT.

1. Introduction

Nanocrystalline (NC) and ultrafine-grained (UFG) materials have been shown to surpass coarse grained materials both in mechanical and in functional utility [1]. During the last couple of decades, severe plastic deformation (SPD) has been used to obtain dense UFG or even NC bulk materials in reasonable volumes [2].

In the majority of the studies SPD processing by high-pressure torsion (HPT) deformation of metal matrix composites (MMCs) showed improved mechanical properties compared to the deformation of pure metals, due to combining matrix and reinforcement properties [3, 4]. These properties are controlled by the size of the reinforcement as well as by its distribution within the matrix [5].

In this study, MMCs with nickel as the metal phase and carbon nanotubes (CNTs) as reinforcement are deformed by HPT. CNTs are well suited for use as reinforcement phase because of their high thermal conductivity, high specific strength, low weight and large aspect ratio [6].

Preinvestigations of SPD deformed Ni and Cu/CNT composites with 1 and 3wt% CNTs and 3 to 4 vol% CNTs have been already performed [7–9]. The present study investigates Ni/CNT MMCs with a greater variety of CNT weight percentages and HPT deformation is additionally conducted at different temperatures to investigate the influence of temperature on the structural evolution. Since CNTs are known to form agglomerates in a metal matrix due to Van der Waals forces [10], a strong emphasis in this study is further laid on obtaining a uniform distribution of small CNT agglomerates. Hence, samples are deformed for different numbers of revolutions as well.

2. Experimental

The initial Ni/CNT MMC material was produced as described in [11]. The samples in the as-fabricated condition had a diameter of 8 mm, a thickness of about 1 mm and contained CNT weight percentages of 0.1, 0.25, 0.5, 1, 2 and 3. These samples were HPT deformed with 0.2 rpm at room temperature (RT) for up to 30 revolutions as described in [12]. Samples were additionally deformed for 30 revolutions at 200°C, 300°C and 400°C with 0.6 rpm, resulting in an equivalent strain of more than 700 at a radius r = 3 mm [13].

Microhardness was measured every 0.25 mm along the radii of the HPT discs (mean value of three indents at each measurement point). The hardness measurements were carried out with a BUEHLER Micromet 5100 using a load of 300 g ($HV_{0.3}$).

Microstructures were characterized in a scanning electron microscope (SEM) type LEO 1525 using back scattered electrons (BSE). Images were taken along the radii of the samples every 0.5 mm to determine the dependence of the microstructural evolution on the equivalent strain. Additionally, HPT deformed samples with 0.1wt% and 1wt% CNTs were prepared for transmission electron microscopy (TEM) investigations (Phillips CM12). HPT deformation parameters were the following: 30 revolutions at 200°C (0.1wt%); 30 revolutions at RT (1wt%); 30 revolutions at 400°C with additional 5 revolutions at RT (1wt%). TEM images were recorded in radial direction for the samples with 1wt% CNTs and in axial direction for the 0.1wt% sample. All TEM samples were obtained at r = 2mm.

3. Results and discussion

With increasing equivalent strain the microhardness increases until it reaches a saturation at high strains for all investigated Ni/CNT MMCs (except the sample containing 3wt% CNTs). This is exemplarily shown in figure 1a for the Ni MMC sample with 1wt% CNTs, which reaches a saturation hardness of 753 HV after 30 revolutions. Independent of the CNT weight percentage, all HPT deformed samples show saturation hardness values above 720 HV after HPT deformation at RT, as can be seen in table 1. The saturation onset for all samples is at a radius of about 3 mm after 30 revolutions, which corresponds to an equivalent strain of about 250 for the Ni/CNT MMC sample containing 1wt% CNTs (figure 1a) and up to an equivalent strain of 400 for other compositions. In pure metals and single phase alloys the saturation regime is reached at a much lower strain [14, 15]. Similar high strains to reach saturation in hardness were needed for HPT-consolidated samples of pure Ni powder [16]. In the Ni/CNT MMCs an additional effect due to the presence of the CNTs has also to be considered. For the sample containing 3wt% CNTs, HPT deformation at RT was limited to 5 revolutions due to the high hardness of the sample. Hence no steady state could be reached in this case.

To investigate the influence of the deformation temperature, HPT samples were deformed at 200°C, 300°C and 400°C. Figure 1b shows the hardness evolution with increasing strain at different deformation temperatures for Ni MMCs with 1wt% CNTs. The sample deformed at 200°C reaches almost the same saturation hardness as the sample deformed at RT, but higher strains are necessary to reach saturation. At 300°C, the saturation hardness decreases to 510 HV. At 400°C, the saturation hardness decreases further (451 HV), but almost the same amount

of strain is needed to reach saturation compared to the sample deformed at RT.
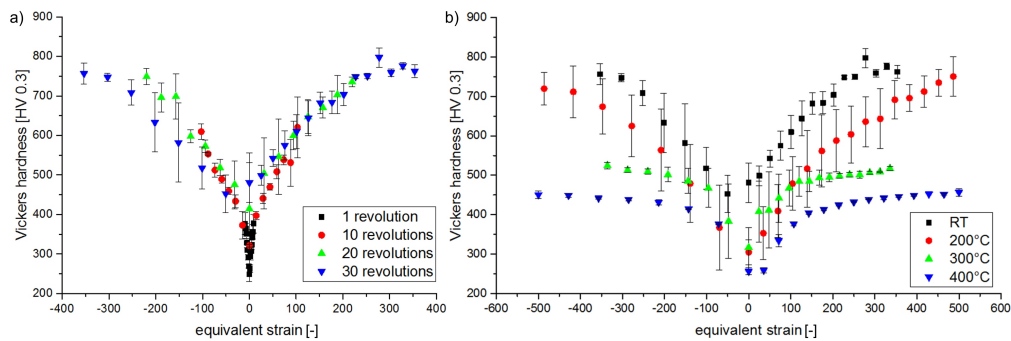
Figure 1. Vickers hardness as function of the applied equivalent strain of Ni MMCs with 1wt% CNTs after a) 1, 10, 20 and 30 revolutions at RT and after b) 30 revolutions at 200°C, 300°C and 400°C.

Table 1 summarizes the saturation hardness values for all compositions and deformation temperatures. For all Ni/CNT MMCs the saturation hardness decreases with increasing deformation temperature. Only for the samples containing 0.5wt% CNTs, nearly the same hardness is reached at RT and 200°C. The Ni/CNT MMC samples with 0.25wt% and 0.5wt% samples have the most distinct decrease in hardness with increasing HPT deformation temperature, the samples containing 2wt% CNTs, the smallest. As an example for the

Table 1. Hardness values for all compositions and deformation temperatures (r = 3 mm).

| wt% CNTs	0.1	0.25	0.5	1	2	3
Saturation hardness RT	729±33	724±33	767±22	753±11	724±24	-
Saturation hardness 200°C	604±19	587±37	762±12	712±49	702±19	776±27
Saturation hardness 300°C	501±5	478±6	520±5	510±6	497±4	600±1
Saturation hardness 400°C	401±3	395±3	438±5	451±3	458±8	465±3

microstructural evolution of the Ni/CNT MMCs with increasing strain, figure 2 shows SEM images of the Ni MMCs with 1wt% CNTs deformed at RT at different amounts of applied strain. The size and the distribution of the CNT agglomerates does not significantly change with increasing number of revolutions, while the grain sizes of the Ni matrix decreases. Surprising is that Ni MMCs with different CNT weight percentages show a similar microstructural evolution of the Ni matrix and CNT distribution independent of the CNT content.

Figure 3 displays the saturation microstructure of the Ni MMCs with 1wt% CNTs at different deformation temperatures recorded at r = 3 mm. With increasing HPT deformation temperature, the saturation grain size increases, while CNT agglomerates become smaller and more globular. After deformation at 300°C the CNTs still show some clustering, although these clusters consist of smaller agglomerates (figure 3c). After deformation at 400°C a homogeneous distribution of small CNT agglomerates is achieved (figure 3d). Ni MMC samples containing higher weight percentages of CNTs show a higher density of agglomerates, but there is no significant influence of CNT content on agglomerate size and shape.

Processing of the Ni MMC samples by HPT leads to strong grain refinement. SEM investigations show a decrease of the grain size with increasing number of revolutions and saturation values
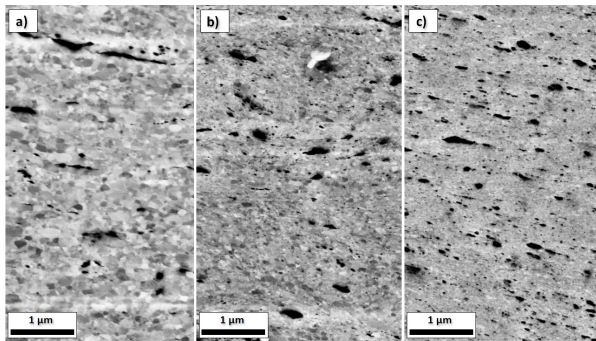
Figure 2. SEM images of Ni MMCs with 1wt% CNTs at r = 3 mm after a) 1, b) 10 and c) 20 revolutions deformed at RT.
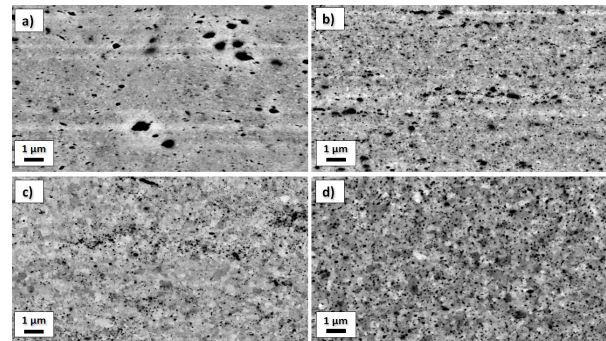
Figure 3. SEM images of Ni MMCs with 1wt% CNTs after 30 revolutions at r = 3 mm at a) RT, b) 200°C, c) 300°C and d) 400°C.

smaller than 40 nm for all compositions after 30 revolutions. However, a slight decrease of the grain size with increasing amount of CNTs is observed.

At a deformation temperature of 200°C, grain sizes increase slightly, but are below 100 nm. For deformation temperatures of 300°C and 400°C grain sizes increase further for nearly all compositions.

Since grains are hardly resolvable in SEM in the saturation region, the microstructure in the steady state of selected samples is additionally investigated in detail by TEM.

Figure 4 shows bright and dark field images with corresponding selected area diffraction (SAD) pattern of the Ni MMC sample with 1wt% CNTs deformed at RT, which was recorded at an equivalent strain of 450. Both images illustrate a nanocrystalline microstructure with grains having a size of about 100 nm and below, showing various defects displayed as contrast variations inside the grains. The grains are clearly elongated along the shear direction (as indicated in figure 4a). In the SAD pattern shown in figure 4a fcc Ni and traces of NiO Debye-Scherrer rings are observed. CNT agglomerates could not be discerned.

The generated microstructures of the Ni MMC sample with the lowest CNT content (0.1wt%) in the saturation regime are shown in bright and dark field images in figure 5. A comparable nanocrystalline structure with few larger but as well very small grains is revealed, where the different grains can hardly be distinguished from each other. The different shape of the grains (equiaxed in this case) is due to the sample being observed in axial direction. In the SAD pattern only fcc Ni rings are visible.
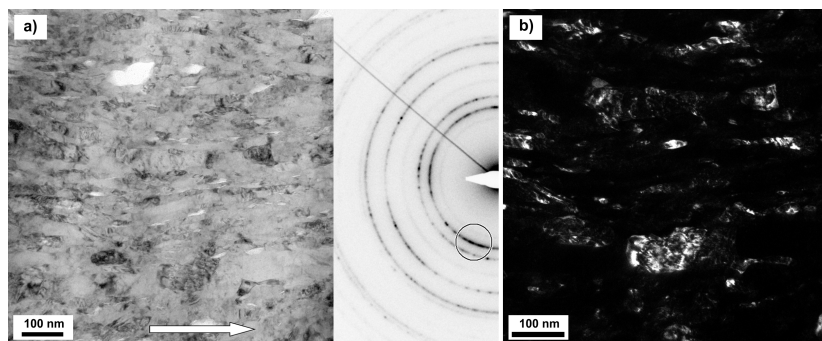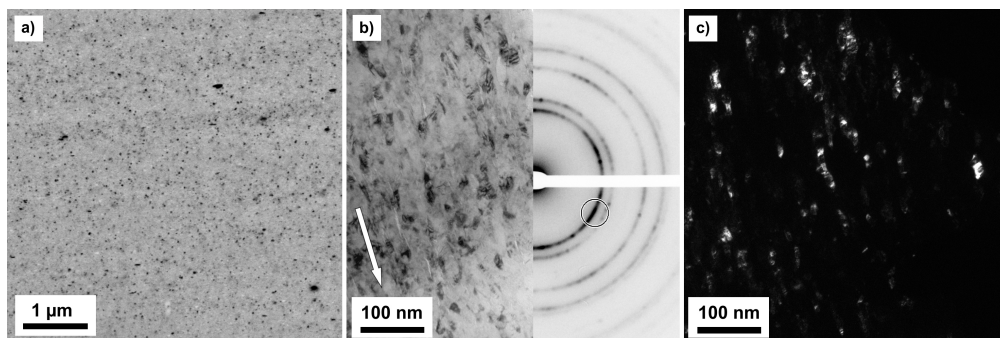

Figure 4. a) Bright field TEM image with corresponding SAD pattern and b) dark field TEM image of Ni MMCs with 1wt% CNTs after 30 revolutions at RT (r = 2 mm). The arrow marks the shear direction.
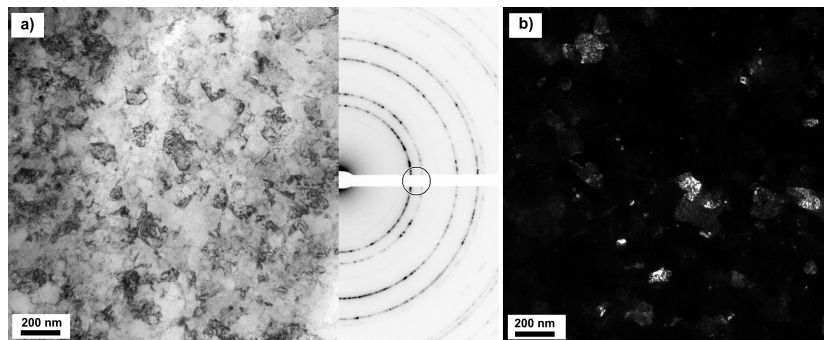
Figure 5. a) Bright field TEM image with corresponding SAD pattern and b) dark field TEM image of Ni MMCs with 0.1wt% CNTs after 30 revolutions at 200°C (r = 2 mm).

Unfortunately, HPT samples deformed at RT show strong crack formation. At deformation temperatures of 300°C and 400°C, no cracks are observed. Furthermore, a better homogeneity of CNT distribution is obtained at 400°C (see figure 3d). A drawback is, however, the decrease of the saturation hardness at this deformation temperature. By contrast, HPT deformation at 200°C prohibits crack formation without significant hardness decrease compared to RT and reduces the grain size compared to 400°C HPT (compare figure 4 and 5).

To achieve a microstructure consisting of a Ni matrix with small grain sizes and small, evenly distributed CNT agglomerates, HPT samples were initially deformed for 30 revolutions at 400°C and subsequently deformed for 5 revolutions at RT. Figure 6 shows the microstructure of a Ni MMC sample with 1wt% CNTs deformed with the aforementioned parameters. In the SEM image (figure 6a) a homogeneous distribution of small, globular CNT agglomerates is visible, while the grains of the Ni matrix are very small. The processed microstructure is also investigated by TEM (figure 6b and c). A nanocrystalline Ni matrix can be seen, in which the grains are below 50 nm in size. The grains are somewhat elongated due to the sample being observed in radial direction (as indicated in figure 6b). Again, no CNT agglomerates could be identified in TEM. The SAD pattern (inset in figure 6b with annotated dark field spot) shows a slight broadening of the Ni diffraction rings, due to the smaller grain size compared to the sample deformed at RT and 200°C (figure 4 and 5). Additionally, weak diffraction rings of NiO are visible.

Figure 6. a) SEM image, b) bright field TEM image with corresponding SAD pattern and c) dark field TEM image of Ni MMC with 1wt% CNTs after 30 revolutions at 400°C and 5 additional revolutions at RT (r = 2 mm). The arrow marks the shear direction.

Ni MMC samples deformed for 30 revolutions at 400°C with additional 5 revolutions at RT exhibit the same crack formation tendency as samples deformed at RT. Hence, HPT parameters

were adjusted to 30 revolutions at 400°C with additional 10 revolutions at 200°C. First microstructural investigations show that comparable microstructures can be achieved using this deformation parameters with the advantage of no crack formation after HPT deformation. Both samples also exhibit the same high hardness of 769 HV. Further adjustments of the HPT parameters and their influence on microstructural evolution are certainly of interest and are currently conducted. For the analysis of the structural defects present in the CNTs after SPD, Raman spectroscopy investigations are underway.

4. Conclusion

Ni MMCs with differing amounts of CNTs were processed by HPT. It could be shown that grain size and microhardness depend strongly on the number of revolutions, while CNT agglomerate size, shape and distribution change only slightly. The applied equivalent strain has a more pronounced effect on the grain size and hardness than the differing weight percentages of CNTs. Increasing the deformation temperature leads to larger grain sizes and a decrease of the hardness in the steady state. CNT agglomerates become smaller, more globular and more evenly distributed with increasing deformation temperature.

Samples, which were deformed for 30 revolutions at 400°C followed by additional 5 revolutions at RT, exhibit the most homogenous microstructure. Crack formation could be prevented by changing the deformation parameters to additional 10 revolutions at 200°C.

References

[1] Gleiter H 1989 *Prog. Mater. Sci.* **33** 223–315
[2] Zhilyaev A P and Langdon T G 2008 *Prog. Mater. Sci.* **53** 893–979
[3] Islamgaliev R K, Buchgraber W, Kolobov Y R, Amirkhanov N M, Sergueeva A V, Ivanov K V and Grabovetskaya G P 2001 *Mater. Sci. Eng. A* **319–21** 872–6
[4] Bachmaier A and Pippan R 2011 *Mater. Sci. Eng. A* **528** 7589–95
[5] Bachmaier A and Pippan R 2013 *Int. Mater. Rev.* **58** 41–62
[6] Jorio A, Dresselhaus G and Gresselhaus M S 2008 *Carbon Nanotubes: Advanced Topics in the Synthesis, Structure, Properties and Applications* (Topics in Applied Physics vol 111) ed C E Ascheron and A H Duhm (Berlin: Springer) chapter 5 pp 165–94
[7] Jenei P, Yoon E Y, Gubicza J, Kim H S, Labar J L and Ungar T 2011 *Mater. Sci. Eng. A* **528** 4690–95
[8] Akbarpour M R, Farvizi M, Lee D J, Rezaei H and Kim H S 2015 *Mater. Sci. Eng. A* **638** 289–95
[9] Suarez S, Lasserre F, Soldera F, Pippan R and Mücklich F 2015 *Mater. Sci. Eng. A* **626** 122–7
[10] Reinert L, Zeiger M, Suarez S, Presser V and Mücklich F 2015 *RSC Adv.* **5** 95149–59
[11] Suarez S, Lasserre F, Prat O and Mücklich F 2014 *Phys. Stat. Sol. A* **211** 1555–61
[12] Hohenwarter A, Bachmaier A, Gludovatz B, Scheriau S and Pippan R 2009 *Int. J. Mater. Res.* **100** 1653–61
[13] Stüwe H P 2003 *Adv. Eng. Mater.* **5**, 291–5
[14] An X H, Lin Q Y, Wu S D, Zhang Z F, Figueiredo R B, Gao N and Langdon T G 2011 *Phil. Mag.* **91:25**, 3307–26
[15] Pippan R, Scheriau S, Taylor A, Hafok M, Hohenwarter A and Bachmaier A 2010 *Annu. Rev. Mater. Res.* **40**, 319–43
[16] Bachmaier A, Hohenwarter A and Pippan R 2009 *Scripta Mater.* **61**, 1016–9